Acoustic black holes, white holes, and wormholes in Bose-Einstein condensates in two dimensions

Sachin Vaidya [*] and Martin Kruczenski [†]
Department of Physics and Astronomy, Purdue University, West Lafayette, Indiana 47907, USA

(Received 22 December 2024; accepted 13 March 2025; published 14 April 2025)

In a previous article, we studied stationary solutions to the dynamics of a Bose-Einstein condensate corresponding to acoustic (or Unruh) black or white holes, namely, configurations where the flow becomes supersonic, creating a horizon for phonons. In this paper, we consider again the Gross-Pitaevskii equation, but looking for stationary numerical solutions in the case where the couplings are position dependent in a prescribed manner. Initially, we consider a two-dimensional quantum gas in a funnel-like spatial metric. We then reinterpret this solution as a solution in a flat metric but with spatially dependent coupling and external potential. In these solutions, the local speed of sound and the magnitude of flow velocity cross, indicating the existence of a supersonic region and therefore of sonic analogs of black and white holes and wormholes. We discuss the numerical techniques used. We also study phase (and density) fluctuations in these solutions and derive approximate acoustic metric tensors. For certain external potentials, we find uniform-density acoustic-black-hole configurations and obtain their Hawking temperature.

DOI: 10.1103/PhysRevA.111.043309

I. INTRODUCTION

In Ref. [1], Unruh proposed the idea of studying acoustic black holes, which can help us to better understand quantum phenomena such as Hawking radiation [2] from the acoustic analog. Such analog gravity models have been theoretically studied extensively [3–8] in the past. Such models have also been studied in a cosmological context (see Refs. [9,10]). In a previous paper [11], we studied stationary singular acoustic-black-hole configurations [in two dimensions (2D)] numerically and through series expansions by finding stationary solutions of the Gross-Pitaevskii equation in 2D with circular symmetry. Asymptotically at infinity the fluid is at rest, but as we approach the origin there is a radially inward flow that becomes supersonic at a certain radius. At that radius, we therefore have an acoustic horizon. Sound cannot escape the supersonic region. Since the fluid accumulates near the origin, we have a singularity in the density that in experiments will be resolved, for example, by three-body recombination (see Refs. [12,13]) or other effects that remove atoms from the condensate. Those solutions were for uniform coupling and no external potential. However, experimental techniques allow for more general cases with external potentials and position-dependent coupling. We can also conceive that future developments allow us to confine the gas to surfaces with nontrivial curvature, allowing for an external nontrivial spatial metric. These techniques can also be used to achieve larger supersonic regions in two-dimensional cases with radial flow (as we shall see), which seems more difficult in general as compared to one-dimensional configurations (see one-dimensional studies [14,15], for example). This is crucial because we need to fit multiple wavelengths of phonons[1] within this region to ensure that it is indeed a black hole, and for further black hole lasing and Hawking radiation studies. In the general case with the spatial metric $\gamma_{ij}(\vec{\mathbf{r}})$, the coupling $g_0(\vec{\mathbf{r}})$, and the external potential $V(\vec{\mathbf{r}})$, the Gross-Pitaevskii equation (GPE) [16] for $\psi(\vec{\mathbf{r}},t) = \sqrt{n(\vec{\mathbf{r}},t)}\exp[i\theta(\vec{\mathbf{r}},t)]e^{-i\mu t}$ reads

$$i\hbar\frac{\partial\psi}{\partial t} = -\frac{\hbar^2}{2m}\frac{1}{\sqrt{\gamma}}\partial_i(\sqrt{\gamma}\gamma^{ij}\partial_j\psi) + g_0(\vec{\mathbf{r}})\,|\psi|^2\,\psi + V(\vec{\mathbf{r}})\psi. \tag{1}$$

If the parameters of the equation and its solution are slowly varying, we can define a local speed of sound [17] as

$$c(\vec{\mathbf{r}},t) = \sqrt{\frac{n(\vec{\mathbf{r}},t)g_0(\vec{\mathbf{r}})}{m}}, \tag{2}$$

where $n = |\psi|^2$ is the density. We can also define a radial flow velocity given by [18]

$$\vec{v}(\vec{\mathbf{r}},t) = \frac{\vec{\mathbf{j}}(\vec{\mathbf{r}},t)}{n(\vec{\mathbf{r}},t)} = \frac{\hbar}{m}\partial^r\theta(\vec{\mathbf{r}},t)\hat{\mathbf{r}}. \tag{3}$$

II. STATIONARY STATES: ACOUSTIC BLACK HOLES, WHITE HOLES, AND WORMHOLES

To get the stationary solutions, we first substitute

$$\psi(\vec{\mathbf{r}},t) = e^{-i\mu t}\phi(\vec{\mathbf{r}},t) \tag{4}$$

[*]Contact author: vaidya2@purdue.edu
[†]Contact author: markru@purdue.edu

[1]Fluctuations in slowly varying background have a nonlinear dispersion relation, linearizing only for long wavelengths, i.e., phonons.

into the GPE (1), and for the purposes of calculation, we scale all equations with

$$T = \mu t, \quad \vec{\mathbf{R}} = \sqrt{\frac{2m\mu}{\hbar}}\vec{\mathbf{r}}, \quad \Phi = \frac{\phi}{\sqrt{\hbar\mu}}, \quad \mathcal{V} = \frac{V}{\hbar\mu}, \tag{5}$$

which turns the Gross-Pitaevskii equation into

$$\Phi + i\frac{\partial\Phi}{\partial T} = -\frac{1}{\sqrt{\gamma}}\partial_i(\sqrt{\gamma}\gamma^{ij}\partial_j\Phi) + g_0(\vec{\mathbf{r}})\,|\Phi|^2\Phi + \mathcal{V}(\vec{\mathbf{r}})\,\Phi. \tag{6}$$

In this work, we consider quantum gases in 2D and use a conformally flat background metric:[2]

$$ds^2 = f(R)[dR^2 + R^2 d\varphi^2], \tag{7}$$

which can also be written as

$$\gamma_{ij} = f(R)\begin{bmatrix} 1 & 0 \\ 0 & R^2 \end{bmatrix}. \tag{8}$$

The GPE (6) in this nontrivial background becomes

$$\Phi + i\frac{\partial\Phi}{\partial T} = -\frac{1}{f(R)}\nabla_R{}^2\Phi + g_0(\vec{\mathbf{R}})|\Phi|^2\Phi + \mathcal{V}(\vec{\mathbf{R}})\Phi, \tag{9}$$

where $\nabla_R{}^2$ is the usual Laplacian and $\Phi = \Phi(T, R, \varphi)$ is the scaled wave function. Further, assuming only radial dependence and replacing

$$\Phi(R) = \rho(R)\exp[i\theta(R)], \tag{10}$$

the imaginary part of the equation gives

$$\frac{\partial\theta}{\partial R} = \frac{B}{R\rho^2}, \tag{11}$$

where B is a constant of integration. Finally, after the substitution (10), the real part of Eq. (9) using Eq. (11) reads

$$\frac{d^2\rho}{dR^2} + \frac{1}{R}\frac{d\rho}{dR} - \frac{B^2}{\rho^3R^2} + f(R)\{[1 - \mathcal{V}(R)]\rho - g_0(R)\rho^3\} = 0. \tag{12}$$

This is the most general form of the static equation that we consider.

Correspondence principle of solutions. Since the form of Eq. (12) depends only on three functions, if we consider two sets of external metrics $f_{1,2}(R)$, potentials $\mathcal{V}_{1,2}(R)$, and couplings $g_{01,02}(R)$ such that

$$f_1(R)[1 - \mathcal{V}_1(R)] = f_2(R)[1 - \mathcal{V}_2(R)], \tag{13}$$

$$f_1(R)\,g_{01}(R) = f_2(R)\,g_{02}(R), \tag{14}$$

then these two sets of functions have the exact same set of solutions for $\rho(R)$. As we see later, unfortunately, this correspondence does not extend to time-dependent fluctuations around these stationary background solutions.

[2]In 2D, any metric can be put in a conformally flat form with an appropriate change of coordinates (see [19] for reference. Also see [20] for application in string theory).

Going back to Eq. (12), since this equation cannot be solved analytically, we solve it using the same boundary-value-problem techniques (Newton iteration with Chebyshev collocation and physics-informed neural networks) we used in Ref. [11] for singular stationary solutions. We also study simpler versions of these solutions in the form of uniform density solutions by introducing a different external potential. Then we study the dynamics of fluctuations in the density and the phase of these solutions under some approximations.

III. ACOUSTIC WORMHOLE SOLUTION

In this section, we consider a case with no external potential and uniform coupling that can be taken as $g_0(R) = 1$ by a rescaling. In this case, we can introduce a scaled local speed of sound of the form

$$C = \frac{\sqrt{2}\rho(R)}{\sqrt{f(R)}} \tag{15}$$

and a scaled flow velocity [from Eq. (11)],

$$\vec{\mathbf{V}}(R) = V^R(R)\hat{\mathbf{R}} = \frac{2\partial_R\theta(R)}{f(R)}\hat{\mathbf{R}} = \frac{2B}{f(R)R[\rho(R)]^2}\hat{\mathbf{R}}. \tag{16}$$

From Eq. (16), it is clear that $B < 0$ corresponds to inward flow and $B > 0$ corresponds to outward flow, and both have the same flow speed for a given $|B|$.

Now we consider

$$f(R) = 1 + \left(\frac{R_0}{R}\right)^4 \tag{17}$$

along with $\mathcal{V}(R) = 0$ and $g_0(R) = 1$ in Eq. (12), giving

$$\frac{d^2\rho}{dR^2} + \frac{1}{R}\frac{d\rho}{dR} + (\rho - \rho^3)\left[1 + \left(\frac{R_0}{R}\right)^4\right] - \frac{B^2}{\rho^3R^2} = 0. \tag{18}$$

The spatial metric $ds^2 = [1 + (\frac{R_0}{R})^4](dR^2 + R^2d\varphi^2)$ transforms to $ds^2 = [1 + (\frac{R_0}{u})^4](du^2 + u^2d\varphi^2)$ under $u = \frac{R_0{}^2}{R}$, which indicates a symmetry about R_0. Equation (18) also clearly exhibits this symmetry and therefore has a similar behavior at $R = 0$ as $R \to \infty$. We look for solutions of the form $\rho(R) \to 1$ as $R \to \infty$, and by symmetry $\rho(R) \to 1$ as $R \to 0$. This metric then describes two separate asymptotic flat regions (see the Appendix) where the fluid flows from one to the other. For that reason, we call this configuration an acoustic wormhole as illustrated in Fig. 1.

A. Numerical solutions

Equation (18) cannot be solved analytically. Therefore, solutions are obtained by using Newton iteration with Chebyshev collocation (with iteration over R_0) as well as using deep learning, as discussed in the case of singular stationary solutions in Ref. [11].

1. Newton iteration with Chebyshev collocation

Here we have a symmetry about R_0, and therefore we need to solve only for $R_0 \leqslant R < \infty$ numerically by mapping it to $[-1, 1]$ as follows:

$$R = R_0 + A\frac{1 + U}{1 - U}, \tag{19}$$

where we choose $A = 10$ to better resolve the structure of the solution. For Chebyshev collocation, we use the collocation

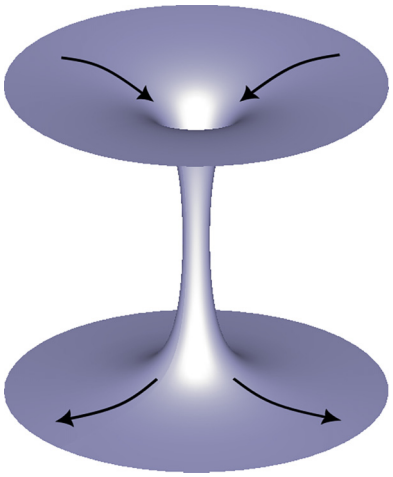

FIG. 1. Theoretical wormhole configuration. The fluid moves along a nontrivial surface connecting two asymptotic regions. The motion is supersonic in the vertical part. In principle, the outer regions can be reconnected to recirculate the subsonic fluid without requiring sources or sinks from the experimental perspective.

grid points given by $U_k = \cos(\frac{\pi k}{N})$, where $k = 0, 1, 2, \ldots, N$. The derivatives are discretized on these grid points using Chebyshev collocation differential matrices (see Ref. [21]).

To construct a Newton method [22] for a boundary value problem, we first write the differential equation (18) in variable U as

$$\text{ODE} = G[\rho(U),\ \rho'(U),\ \rho''(U)] = 0,$$
$$\text{where} \quad \rho'(U) = \frac{d\rho(U)}{dU}, \quad \rho''(U) = \frac{d^2\rho(U)}{dU^2}, \tag{20}$$

and we expand G in Eq. (20) about $\rho_{\text{old}}(U)$ at first order [23]:

$$G_{\text{old}} + (\rho_{\text{new}} - \rho_{\text{old}})\left(\frac{dG}{d\rho}\bigg|_{\rho=\rho_{\text{old}}}\right) + (\rho'_{\text{new}} - \rho'_{\text{old}})\left(\frac{dG}{d\rho'}\bigg|_{\rho'=\rho'_{\text{old}}}\right) + (\rho''_{\text{new}} - \rho''_{\text{old}})\left(\frac{dG}{d\rho''}\bigg|_{\rho''=\rho''_{\text{old}}}\right) = 0. \tag{21}$$

We use Eq. (21) along with Chebyshev collocation differential matrices to implement the Newton iteration (in C++) with mixed boundary conditions $\rho'(U = -1) = 0$ and $\rho(U = 1) = 1$. This can be easily achieved by adding a row for the derivative at the left boundary (at R_0) in the rectangular matrix of the system of $N - 1$ discretized equations in N unknowns. Then these Newton iterations are performed with some initial guess of the function as well as R_0 until the iteration error becomes small enough and falls within the acceptable numerical error. It is interesting to note that the solutions obtained using this approach turn out to have a lower bound on the value of R_0 for a given value of the parameter[3] $|B|$. A sample solution is shown in Fig. 2 and plotted against a corresponding singular stationary solution from Ref. [11] to show how this model provides a regularization of the singular solutions discussed in Ref. [11].

[3] $B < 0$ and $B > 0$ have the same solutions for a given $|B|$.

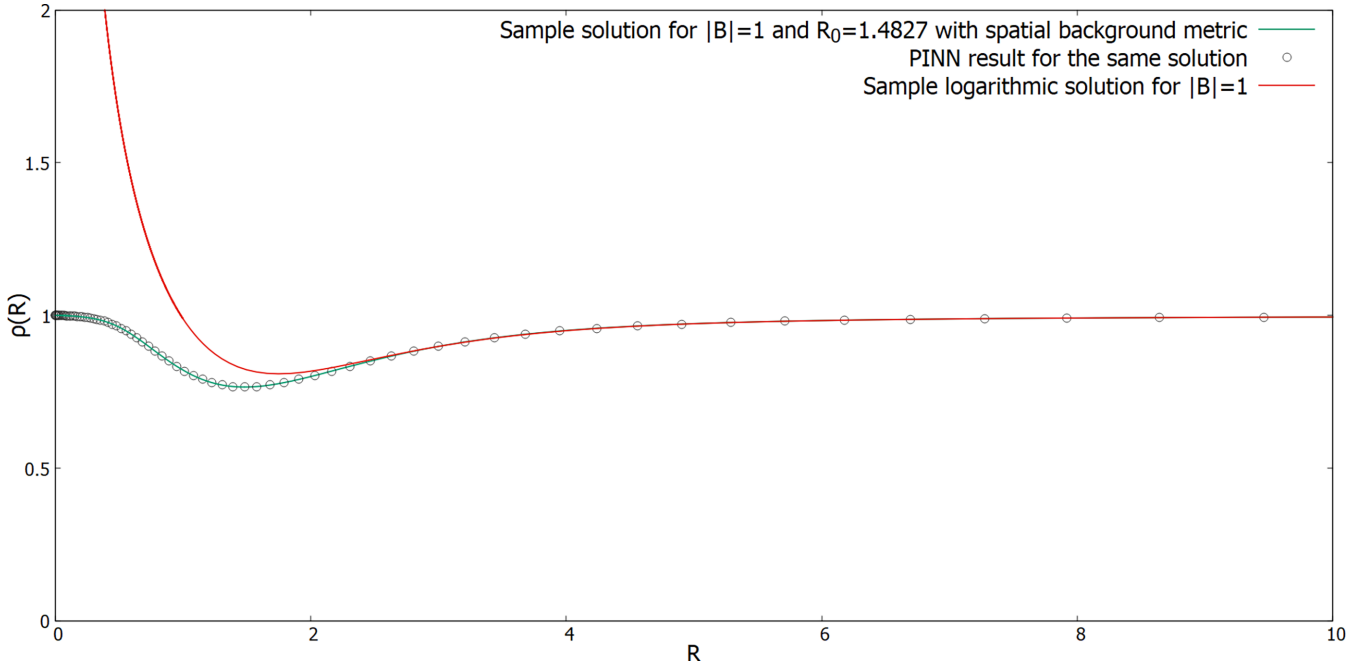

FIG. 2. Sample solution with background metric compared with logarithmic singular solution for $|B| = 1$ in 2D. The neural network result for the same solution is shown in circles.

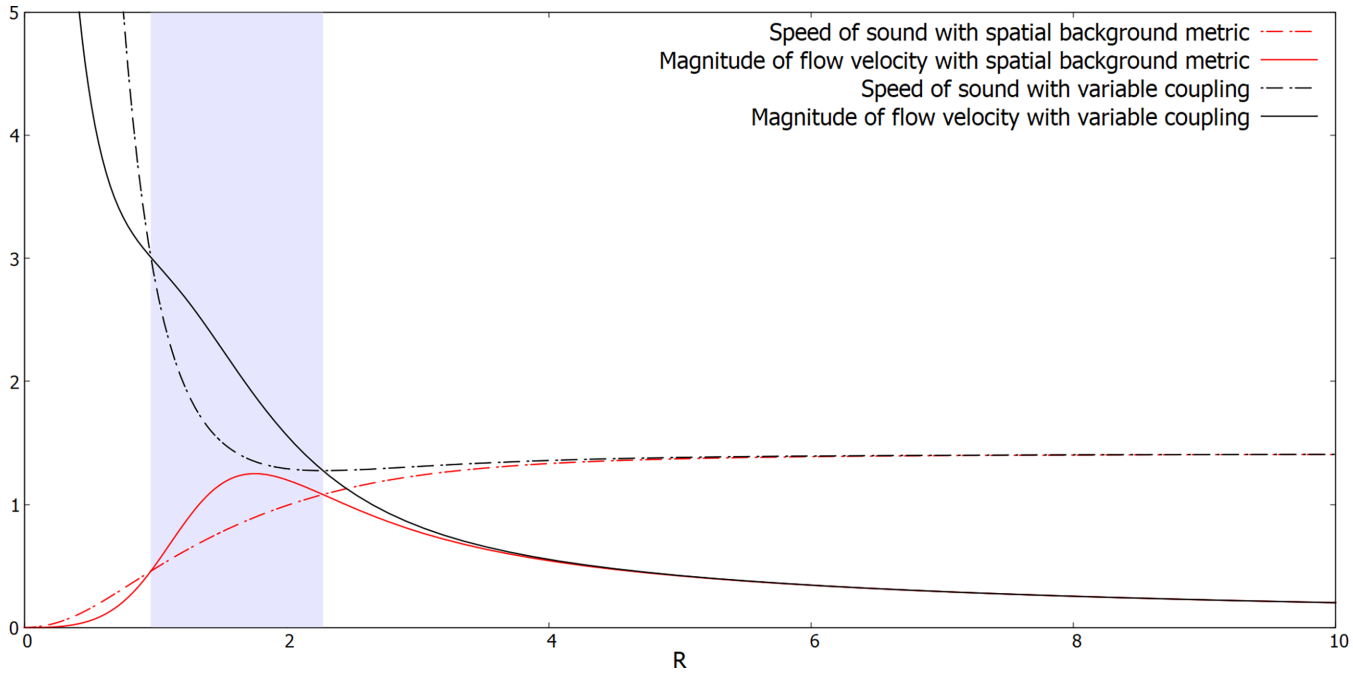

FIG. 3. Speed of sound (dashed line) and magnitude of flow velocity (solid line) for $|B| = 1$ and $R_0 = 1.4827$ with background metric (in red) and variable coupling (in black) in 2D with supersonic region in blue shade.

2. *Physics-informed neural network.*

This problem can also be solved using neural networks. We employ the same neural network[4] we used in Ref. [11] except that now we map $R \in [0, \infty] \to U \in [-1, 1]$, with $R = R_0 \frac{1+U}{1-U}$. We scale the unknown function as $1 - 0.1(1 - U^2)^2 N(U, P)$ so that the only unknown is the neural network $N(U, P)$ and the function and its slope are always 1 and 0, respectively, at both boundaries. The result of this for the same solution obtained earlier with the Newton method is shown in circles in Fig. 2.

Figure 3 shows the speed of sound and the magnitude of the flow velocity for this solution with a background funnel metric clearly indicating a crossover between the speed of sound and the magnitude of flow velocity and thus the existence of a supersonic region and, therefore, a sonic black or white hole. Since Eq. (18) and by extension its solution exhibit symmetry about R_0, regions $R \to \infty$ and $R \to 0$ represent two identical asymptotically uniform density regions. Therefore, this black or white hole can be thought of as an acoustic (one-way) wormhole (see Fig. 1), as we shall see.

B. Fluctuations and acoustic wormhole metric

Fluctuations of these solutions satisfy Eq. (9) with $\mathcal{V}(R) = 0$ and $g_0(R) = 1$. Introducing density and phase perturbations of the form

$$\begin{aligned}
&\Phi(R, \varphi, T) \\
&= \sqrt{n(R, \varphi, T)} \exp[i\theta(R, \varphi, T)] \\
&= \sqrt{n_0(R) + n_1(R, \varphi, T)} \exp\{i[\theta_0(R) + \theta_1(R, \varphi, T)]\} \\
&\approx \sqrt{n_0(R)} \exp[i\theta_0(R)] \left(1 + \frac{n_1(R, \varphi, T)}{2n_0(R)} + i\theta_1(R, \varphi, T)\right) \\
&= \sqrt{n_0(R)} \exp[i\theta_0(R)][1 + N_1(R, \varphi, T) + i\theta_1(R, \varphi, T)],
\end{aligned} \tag{22}$$

where $n_0(R) = [\rho_0(R)]^2$ and $\theta_0(R)$ are the background density and phase, we get the following linearized coupled equations that govern the dynamics of density and phase perturbations:

$$\begin{aligned}
&\left(\partial_T - \frac{2|B|}{f(R)R[\rho_0(R)]^2}\partial_R\right) N_1(R, \varphi, T) \\
&\quad = -\frac{1}{f(R)\rho_0(R)^2} \nabla_R \cdot [\rho_0(R)^2 \nabla_R \theta_1(R, \varphi, T)],
\end{aligned} \tag{23}$$

$$\begin{aligned}
&\left(\partial_T - \frac{2|B|}{f(R)R[\rho_0(R)]^2}\partial_R\right) \theta_1(R, \varphi, T) \\
&\quad = \frac{1}{f(R)\rho_0(R)^2} \nabla_R \cdot [\rho_0(R)^2 \nabla_R N_1(R, \varphi, T)] \\
&\qquad - 2\rho_0(R)^2 N_1(R, \varphi, T),
\end{aligned} \tag{24}$$

where $N_1(R, \varphi, T) = \frac{n_1(R,\varphi,T)}{2n_0(R)} = \frac{n_1(R,\varphi,T)}{2[\rho_0(R)]^2}$.

Under the hydrodynamic approximation $\nabla_R \cdot [\rho_0(R)^2 \nabla_R N_1(R, \varphi, T)] \approx 0$ (see Refs. [4,5]), Eqs. (23) and (24) can be combined, and the result looks like a massless scalar field $\theta_1(R, \varphi, T)$ in an acoustic (space-time) metric background (see Ref. [24]). The acoustic metric here

[4]1, 15, 20, 15, and 1 neuron in each layer from input to output layers, with Adam optimizer, and tanh activation function, as well as PYTHON library PYTORCH along with the automatic differentiation engine called autograd.

looks like the Schwarzschild metric in Painlevé-Gullstrand coordinates (see Ref. [25]).

$$g_{\mu\nu} \sim \rho_0(R)^4 \begin{bmatrix} -\left(1-\frac{2B^2R^2}{\rho_0(R)^6\left(R^4+R_0^4\right)}\right) & \frac{|B|}{R\rho_0(R)^4} & 0 \\ \frac{|B|}{R\rho_0(R)^4} & \frac{R^4+R_0^4}{2R^4\rho_0(R)^2} & 0 \\ 0 & 0 & \frac{R^4+R_0^4}{2R^2\rho_0(R)^2} \end{bmatrix}. \tag{25}$$

Here, condensate flows with a subsonic flow from an asymptotically flat region at $R \to \infty$ to an identical asymptotically flat region at $R \to 0$ (see the Appendix), with the flow becoming supersonic in some neighborhood of R_0. This looks like a (one-way) wormhole (see Fig. 1) connecting two patches of this analog space-time.[5]

IV. UNIFORM-DENSITY WORMHOLES

It is interesting to note that allowing for an external potential together with a spatial metric allows for a special class of solutions with uniform density. Indeed, setting $g_0(R) = 1$ and $\rho(R) = 1$ in Eq. (12), we get

$$-\frac{B^2}{R^2} - f(R)\mathcal{V}(R) = 0. \tag{26}$$

Therefore, such solutions exist if the potential satisfies this condition, giving

$$\mathcal{V}(R) = -\frac{B^2}{R^2\left[1+\left(\frac{R_0}{R}\right)^4\right]} \tag{27}$$

for the case we are considering here where $f(R)$ is given by Eq. (17). With $\rho = 1$, from Eqs. (15) and (16), the flow velocity becomes $\vec{\mathbf{V}}(R) = \frac{2B}{f(R)R}\hat{\mathbf{R}}$ and the local speed of sound becomes $C = \frac{\sqrt{2}}{\sqrt{f(R)}}$. For some sample solutions the flow speed and the sound speed are shown in Fig. 4. The advantage of this solution is that the exact location R_h of the acoustic horizons is known in a closed form, $R_h = \sqrt{B^2 \pm \sqrt{B^4 - {R_0}^4}}$.

A. Fluctuations and acoustic wormhole metric

It can be shown in a way similar to that in the previous section that the perturbations of this background solution also look like a massless scalar field in an acoustic (space-time) metric background [from Eq. (25)] in the hydrodynamic limit, and the acoustic metric looks as follows:

$$g_{\mu\nu} \sim \begin{bmatrix} -\left(1-\frac{2B^2R^2}{\left(R^4+R_0^4\right)}\right) & \frac{|B|}{R} & 0 \\ \frac{|B|}{R} & \frac{R^4+R_0^4}{2R^4} & 0 \\ 0 & 0 & \frac{R^4+R_0^4}{2R^2} \end{bmatrix}, \tag{28}$$

which also looks like a wormhole (see Fig. 1) similar to nonuniform-density configurations discussed in the previous section.

[5]We consider solutions with $B < 0$. It is a one-way wormhole because phonons can cross the horizons only in one direction.

B. Hawking temperature from fluctuations in the hydrodynamic limit with $R_0 \approx 0$

In the limit of $R_0 \approx 0$, this system looks like the one discussed in Ref. [26] for a photon gas. This system has only one horizon given by $R_h = \sqrt{2}|B|$. Furthermore, $R_0 \approx 0$ gives the flow velocity $\vec{\mathbf{V}}(R) \approx \frac{2B}{R}\hat{\mathbf{R}}$ and the local speed of sound $C \approx \sqrt{2}$ from Eqs. (16) and (15), respectively.

1. Bogoliubov transform

Thinking of phase perturbations (under the hydrodynamic approximation) as a massless scalar field in the acoustic metric background given by Eq. (28) with $R_0 \approx 0$, we can reproduce the system discussed in Ref. [26]. Thus, from Ref. [26] we get the temperature T_H of this analog black hole to be $T_H = \frac{1}{2\pi|B|}$.

2. Analytic continuation

One more check is to analytically continue the outgoing solution in the vicinity of the horizon from outside to inside.[6] It can be shown that the radial dependence of the outgoing solution near the horizon has the form $(R - \sqrt{2}|B|)^{i\omega|B|}$. Therefore, we get a real exponential correction inside the horizon $e^{|B|\omega\pi}$. This gives the ratio $e^{-2|B|\omega\pi}$ (where $\omega > 0$) of the squared amplitude of the outgoing solution outside and inside the horizon, similar to the relation between Bogoliubov coefficients [26]. This can also be thought of as a tunneling probability (< 1) or tunneling coefficient for the analog Hawking radiation (similar to Ref. [27] except in Painlevé-Gullstrand coordinates). This is consistent with the previous approach.

3. Periodicity of Wick-rotated Euclidean time

Furthermore, if we diagonalize the acoustic metric (28) (with $R_0 = 0$) by combining coordinates T and R into a new time coordinate $T_{\rm sch}$, the metric becomes

$$ds^2 = -\frac{\left(R^2-R_h^2\right){dT_{\rm sch}}^2}{R^2} + \frac{R^2dR^2}{2\left(R^2-R_h^2\right)} + \frac{R^2}{2}d\varphi^2, \tag{29}$$

where $R_h = \sqrt{2}|B|$ in Eq. (29). Under the coordinate transformation $R = R_h + \frac{1}{\sqrt{2}|B|}\epsilon^2$, the temporal and radial parts of the metric become

$$-\frac{\epsilon^2{dT_{\rm sch}}^2}{B^2} + d\epsilon^2, \tag{30}$$

where through Wick rotation, if we redefine $\beta = i\frac{T_{\rm sch}}{|B|}$, to avoid a conical singularity, β should have periodicity 2π and therefore the temperature is $T_H = \frac{1}{2\pi|B|}$, which gives the tunneling coefficient $e^{-2|B|\omega\pi}$. This is consistent with the previous approaches that we discussed.

[6]The coordinates need to be smooth across the horizon, which is the case with the Painlevé-Gullstrand-like coordinates used.

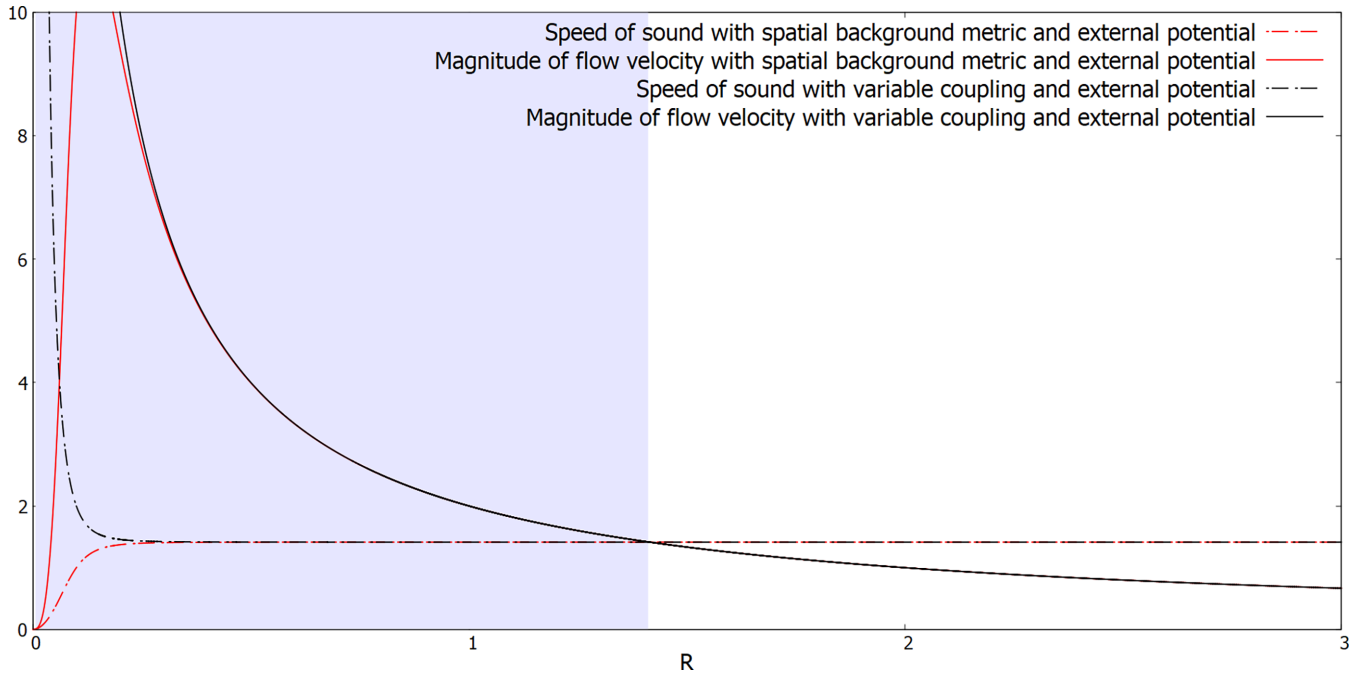

(a) $|B| = 1.0$ and $R_0 = 0.1$

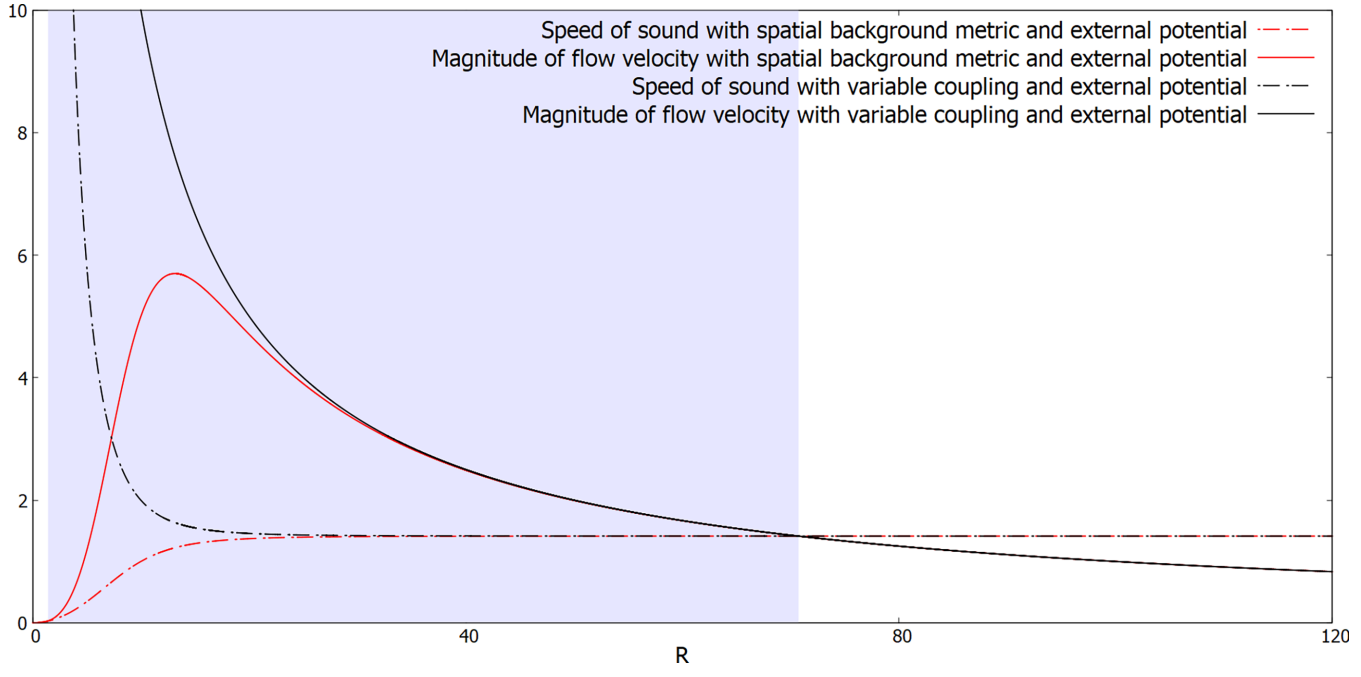

(b) $|B| = 50.0$ and $R_0 = 10.0$

FIG. 4. Speed of sound (dashed line) and magnitude of flow velocity (solid line) for sample solutions with background metric (in red) and variable coupling (in black) as well as external potential in 2D with the supersonic region in blue shade.

C. Hawking temperature from fluctuations in the hydrodynamic limit with $R_0 \neq 0$

Now if we go back to Eq. (28) and consider $R_0 \neq 0$, there are two horizons given by $R_{p,m} = \sqrt{B^2 \pm \sqrt{B^4 - {R_0}^4}}$ (in the extremal case $|B| = R_0$). Since there is no exact solution for the massless scalar filed $\theta_1(R, \varphi, T)$ even in the hydrodynamic approximation, we just study the equation in the vicinity of the outer horizon.

1. Analytic continuation

One method is to analytically continue the solution in the vicinity of the outer horizon from the outside to the inside.[6] The radial dependence of the solution near the outer horizon R_p is of the form $(R - R_p)^{\frac{i\omega|B|^3}{\sqrt{B^4-R_0{}^4}}}$. Therefore, we get real exponential corrections of the form $e^{-\frac{\pi(R_m^2+R_p^2)^{\frac{3}{2}}\omega}{\sqrt{2}(R_p^2-R_m^2)}} =$

$e^{-\frac{\pi|B|^3\omega}{\sqrt{B^4-R_0^4}}}$ while going from inside to outside R_p. The ratio of amplitude squared outside to amplitude squared inside can be interpreted as the semiclassical probability of tunneling (< 1) or the tunneling coefficient (similar to Ref. [27] except in Painlevé-Gullstrand coordinates), giving the temperature $T_H = \frac{\sqrt{2}(R_p^2-R_m^2)}{2\pi(R_m^2+R_p^2)^{\frac{3}{2}}} = \frac{\sqrt{B^4-R_0^4}}{2\pi|B|^3}$.

2. Periodicity of Wick-rotated Euclidean time

If we diagonalize the acoustic metric (28) by combining coordinates T and R into a new time coordinate $T_{\rm sch}$, the metric becomes

$$ds^2 = -\frac{(R^2-R_p^2)(R^2-R_m^2)dT_{\rm sch}{}^2}{R^4+R_p^2R_m^2} + \frac{(R^4+R_p^2R_m^2)^2dR^2}{2R^4(R^2-R_p^2)(R^2-R_m^2)} + \frac{(R^4+R_p^2R_m^2)d\varphi^2}{2R^2}, \tag{31}$$

where $R_p = \sqrt{B^2+\sqrt{B^4-R_0{}^4}}$ and $R_m = \sqrt{B^2-\sqrt{B^4-R_0{}^4}}$. Under the coordinate transformations near R_p given by $R = R_p + \frac{(R_p^2-R_m^2)R_p}{(R_p^2+R_m^2)^2}\epsilon^2 = R_p + \frac{\sqrt{B^4-R_0^4}(B^2+\sqrt{B^4-R_0^4})}{2|B|^4}\epsilon^2$, the temporal and radial parts of the metric become

$$\text{At } R_p \Rightarrow -\frac{2\left(-R_m^2+R_p^2\right)^2}{\left(R_m^2+R_p^2\right)^3}\epsilon^2 dT_{\rm sch}{}^2 + d\epsilon^2 = -\frac{B^4-R_0^4}{B^6}\epsilon^2 dT_{\rm sch}{}^2 + d\epsilon^2, \tag{32}$$

where through Wick-rotated Euclidean time and its periodicity of 2π, we get the temperature at the outer black-hole horizon,

$$T_H = \frac{\sqrt{2}\left(R_p^2-R_m^2\right)}{2\pi\left(R_m^2+R_p^2\right)^{\frac{3}{2}}} = \frac{\sqrt{B^4-R_0^4}}{2\pi|B|^3}. \tag{33}$$

This gives the tunneling coefficient across the outer horizon as

$$e^{-\frac{2\pi\omega(R_m^2+R_p^2)^{\frac{3}{2}}}{\sqrt{2}(R_p^2-R_m^2)}} = e^{-\frac{2\pi\omega|B|^3}{\sqrt{B^4-R_0^4}}}. \tag{34}$$

This is consistent with the analytic continuation across the horizon.

V. RADIALLY VARYING COUPLING AND EXTERNAL POTENTIAL

In a laboratory setting, a nontrivial background metric can be accomplished by restricting the fluid to move on a curved surface rather than a flat one. Although this might be possible, we point out in this section that the solution corresponding to the spatial funnel metric in Sec. III can be reinterpreted as a solution in a spatial flat metric by using the correspondence principle discussed in Sec. II. Instead of $f(R)$, $\mathcal{V}(R)$, and $g_0 = 1$, we can use a flat metric with the potential $U(R)$ and the coupling $g_0(R)$ such that

$$U(R) - 1 = [\mathcal{V}(R) - 1]f(R), \tag{35}$$

$$g_0(R) = f(R), \tag{36}$$

where $f(R) = 1 + (\frac{R_0}{R})^4$. Both of these configurations (on the left and the right above) have identical stationary solutions. Notice that, with the funnel metric, the region near $R = 0$ was interpreted as another asymptotic region, as is evident from the symmetry between large and small R. The incoming flux from one region goes out through the other region. On the other hand, in the corresponding flat metric with the variable coupling case, $R = 0$ represents the origin of the plane and the fluid appears to have nowhere to go. By carefully looking at the GPE, one can see that the solution corresponds to a GPE with a sink at the center that removes the atoms, which can be simulated by an imaginary Dirac δ-function potential at $R = 0$. This is also reflected in the fact that the scaled local speed of sound is now $C = \sqrt{2f(R)}\rho(R)$ and the flow velocity is $\vec{\mathbf{V}}(R) = \frac{2B}{R[\rho(R)]^2}\hat{\mathbf{R}}$. They are singular when $R \to 0$ (see Fig. 3) despite the fact that the amplitude or density of the stationary solution itself is well behaved (see Fig. 2). This breaks the symmetry about R_0, which is also evident from the equations that govern fluctuations, as we see in the next subsection.

Fluctuations

Introducing perturbation in the stationary solution as was done earlier (22), we find

$$\left(\partial_T - \frac{2|B|}{R[\rho_0(R)]^2}\partial_R\right)N_1(R,\varphi,T) = -\frac{1}{\rho_0(R)^2}\nabla_R\cdot[\rho_0(R)^2\nabla_R\theta_1(R,\varphi,T)], \tag{37}$$

$$\left(\partial_T - \frac{2|B|}{R[\rho_0(R)]^2}\partial_R\right)\theta_1(R,\varphi,T) = \frac{1}{\rho_0(R)^2}\nabla_R\cdot[\rho_0(R)^2\nabla_R N_1(R,\varphi,T)] - 2f(R)\rho_0(R)^2N_1(R,\varphi,T), \tag{38}$$

where $N_1(R,\varphi,T) = \frac{n_1(R,\varphi,T)}{2n_0(R)} = \frac{n_1(R,\varphi,T)}{2[\rho_0(R)]^2}$. We notice that Eqs. (37) and (38) clearly differ from Eqs. (23) and (24). In addition, Eqs. (37) and (38) lack the symmetry about R_0 that Eqs. (23) and (24) enjoy. Now we proceed to analyze the solutions.

Under the hydrodynamic approximation $\nabla_R\cdot[\rho_0(R)^2\nabla_R N_1(R,\varphi,T)] \approx 0$, Eqs. (37) and (38) can be combined, and the result looks like a massless scalar field $\theta_1(R,\varphi,T)$ in an acoustic (space-time) metric background (see Ref. [24]). The acoustic metric here looks like the Schwarzschild metric in Painlevé-Gullstrand coordinates (see

Ref. [25]):

$$g_{\mu\nu} \sim \rho_0(R)^4 \begin{bmatrix} -\left(1-\frac{2B^2R^2}{\rho_0(R)^6(R^4+R_0^4)}\right) & \frac{|B|R^3}{(R^4+R_0^4)\rho_0(R)^4} & 0 \\ \frac{|B|R^3}{(R^4+R_0^4)\rho_0(R)^4} & \frac{R^4}{2(R^4+R_0^4)\rho_0(R)^2} & 0 \\ 0 & 0 & \frac{R^6}{2(R^4+R_0^4)\rho_0(R)^2} \end{bmatrix}. \tag{39}$$

This acoustic metric tensor clearly lacks the symmetry about R_0 and it no longer corresponds to a (one-way) wormholelike configuration because it lacks a second asymptotic region at $R = 0$.

VI. UNIFORM DENSITY SOLUTION WITH RADIALLY VARYING COUPLING AND EXTERNAL POTENTIALS

From Eq. (12) we find that there are uniform density solutions $\rho = 1$ with no external metric if the condition

$$-\frac{B^2}{R^2} + [1 - \mathcal{V}(R) - g_0(R)] = 0 \tag{40}$$

is satisfied. Using the correspondence principle of Sec. II, we find this case can be related to the nontrivial metric $f(R)$, the potential $\tilde{\mathcal{V}}(R)$, and constant coupling if

$$[1 - \mathcal{V}(R)] = f(R)[1 - \tilde{\mathcal{V}}(R)], \tag{41}$$

$$g_0(R) = f(R). \tag{42}$$

Therefore, setting

$$g_0(R) = 1 + \left(\frac{R_0}{R}\right)^4 \tag{43}$$

and the potential according to Eq. (40), we find uniform density solutions with a nontrivial acoustic metric for the fluctuations as discussed in the next subsection. Furthermore, the local speed of sound and the flow velocity become $C = \sqrt{2f(R)}$ and $\vec{\mathbf{V}}(R) = \frac{2B}{R}\hat{\mathbf{R}}$, respectively, which as shown in Fig. 4 are clearly singular[7] despite the $\rho(R)$ of the stationary background solution being 1 everywhere. These are perhaps the solutions that are easier to reproduce in an experimental setting.

A. Fluctuations

It can be shown in a way similar to that in the previous section that the perturbations in this background solution also look like a massless scalar field in an acoustic (space-time) metric background [from Eq. (39)] in the hydrodynamic limit, and the acoustic metric looks as follows:

$$g_{\mu\nu} \sim \begin{bmatrix} -\left(1-\frac{2B^2R^2}{(R^4+R_0^4)}\right) & \frac{|B|R^3}{(R^4+R_0^4)} & 0 \\ \frac{|B|R^3}{(R^4+R_0^4)} & \frac{R^4}{2(R^4+R_0^4)} & 0 \\ 0 & 0 & \frac{R^6}{2(R^4+R_0^4)} \end{bmatrix}. \tag{44}$$

[7]The inner horizon is excluded from the plot because it is way outside the bounds of the plot. This is because sound and flow speeds are singular as discussed.

This metric tensor also clearly lacks the symmetry about R_0 and it no longer corresponds to a wormhole, because it lacks a second asymptotic region.

B. Hawking temperature from fluctuations in the hydrodynamic limit with $R_0 \approx 0$

In the limit of $R_0 \approx 0$, metric tensors (44) and (28) look exactly the same, and therefore with $R_0 \approx 0$ this system also looks like the one discussed in Ref. [26] for the photon gas and therefore the solutions of the perturbation equations exhibit the same behavior as discussed for the uniform-density solution with spatial background funnel metric and external potential. Therefore, the temperature is $T_H = \frac{1}{2\pi|B|}$, which gives the tunneling coefficient $e^{-2|B|\omega\pi}$.

C. Hawking temperature from fluctuations in the hydrodynamic limit with $R_0 \neq 0$

Now, if we go back to Eq. (44) and consider $R_0 \neq 0$, there are two horizons given by $R_{p,m} = \sqrt{B^2 \pm \sqrt{B^4 - {R_0}^4}}$ (in the extremal case $|B| = R_0$), but again there is no exact solution for the massless scalar $\theta_1(R, \varphi, T)$ even in the hydrodynamic approximation. However, we can still analyze the behavior near the outer horizon as follows.

1. Analytic continuation

One can analytically continue the solution in the vicinity of the outer horizon from the outside to the inside.[6] In this case, the solution near the outer horizon R_p has the radial dependence of the form $(R - R_p)^{\frac{i\omega|B|(B^2+\sqrt{B^4-{R_0}^4})}{2\sqrt{B^4-{R_0}^4}}}$. Therefore, we get real exponential corrections while going from outside to inside R_p. The ratio of the modulus square of the solution outside and inside the horizon can be interpreted as a tunneling coefficient (similar to Ref. [27] except in Painlevé-Gullstrand coordinates) or the probability of tunneling (< 1). This indicates the temperature $T_H = \frac{\sqrt{2}(R_p^2 - R_m^2)}{2\pi\sqrt{R_m^2 R_p^2 R_p^2}} = \frac{2\sqrt{B^4-R_0^4}}{2\pi|B|(B^2+\sqrt{B^4-R_0^4})}$.

2. Periodicity of Wick-rotated Euclidean time

If we diagonalize the acoustic metric (44) by combining coordinates T and R into a new time coordinate T_{sch}, the metric becomes

$$ds^2 = -\frac{(R^2 - R_p^2)(R^2 - R_m^2)dT_{\text{sch}}{}^2}{R^4 + R_p^2 R_m^2} + \frac{R^4 dR^2}{2(R^2 - R_p^2)(R^2 - R_m^2)} + \frac{R^6}{2R^4 + 2R_p^2 R_m^2} d\varphi^2, \tag{45}$$

where $R_p = \sqrt{B^2 + \sqrt{B^4 - {R_0}^4}}$ and $R_m = \sqrt{B^2 - \sqrt{B^4 - {R_0}^4}}$. Under the coordinate transformations near R_p given by $R = R_p + \frac{Rp^2 - R_m^2}{R_p^3}\epsilon^2 = R_p + \frac{2\sqrt{B^4 - R_0^4}}{(B^2 + \sqrt{B^4 - R_0^4})^{\frac{3}{2}}}\epsilon^2$, the temporal and radial parts of the metric become

$$\text{at } R_p \Rightarrow -\frac{2\left(-R_m^2 + R_p^2\right)^2}{R_p^4\left(R_m^2 + R_p^2\right)}\epsilon^2 {dT_{\text{sch}}}^2 + d\epsilon^2 = \frac{-\left(4B^4 - 4R_0^4\right)}{\left(B^2 + \sqrt{B^4 - R_0^4}\right)^2 B^2}\epsilon^2 {dT_{\text{sch}}}^2 + d\epsilon^2, \tag{46}$$

where through Wick-rotated Euclidean time (see the process explained in Ref. [28]) and its periodicity of 2π we get the temperature at the outer black-hole horizon

$$T_H = \frac{\sqrt{2}\left(R_p^2 - R_m^2\right)}{2\pi R_p^2\sqrt{R_m^2 + R_p^2}} = \frac{2\sqrt{B^4 - R_0^4}}{2\pi\left(B^2 + \sqrt{B^4 - R_0^4}\right)|B|}. \tag{47}$$

This gives a tunneling coefficient,

$$e^{-\frac{2\pi\omega R_p^2\sqrt{R_m^2 + R_p^2}}{\sqrt{2}(R_p^2 - R_m^2)}} = e^{-\frac{2\pi\omega(B^2 + \sqrt{B^4 - R_0^4})|B|}{2\sqrt{B^4 - R_0^4}}}, \tag{48}$$

consistent with the analytic continuation across the horizon.

VII. CONCLUSIONS

We obtained nonsingular stationary solutions of the Gross-Pitaevskii equation by putting a spatial funnel-like metric describing a space with two asymptotic regions. The fluid moves radially inwards in one region and comes out in the other one. Therefore the fluid does not accumulate and no singularity is produced. The spatial funnel-metric is particularly interesting because it resembles a (one-way) wormhole for phonons in the hydrodynamic limit. We also obtained nonsingular stationary solutions of the Gross-Pitaevskii equation using position-dependent coupling and potential. We expect this latter approach to be more feasible in actual experiments. In this approach, we do not see a wormholelike behavior, but we still do get acoustic black-hole or white-hole configurations. Perhaps the most interesting configurations from a practical point of view are ones with uniform density that appear when the funnel metric or the position-dependent coupling and potential are related to each other in a particular way. Additionally, since these uniform-density configurations can be made to have an arbitrarily large supersonic region, multiple phonon wavelengths can be fit into the region, making it more feasible to study black-hole lasing and Hawking radiation.

In all the configurations discussed, the approximate local speed of sound and the magnitude of flow velocity cross. That means we do indeed find acoustic black-hole, white-hole, and wormhole configurations. We also see that, in the hydrodynamic limit, the phase fluctuations around the stationary solutions behave as a massless scalar (phonon) field in an acoustic metric background. In particular, the fluctuations around the uniform density solutions are easy to analyze, leading to specific values for the black-hole temperature.

ACKNOWLEDGMENTS

We are grateful to the DOE for support under the Fermilab Quantum Consortium. We are grateful to Dr. Sergei Khlebnikov and Dr. Chen-Lung Hung for various comments and discussions. We also wish to acknowledge valuable computational resources provided by RCAC (Rosen Center for Advanced Computing) at Purdue University.

DATA AVAILABILITY

No data were created or analyzed in this study.

APPENDIX: ACOUSTIC WORMHOLE DOUBLE-FUNNEL

In Sec. III, we consider a 2D quantum fluid in a conformally flat metric given by

$$ds^2 = f(R)\,(dR^2 + R^2 d\theta^2), \quad f(R) = 1 + \frac{R_0^4}{R^4}. \tag{A1}$$

To potentially recreate such a metric in a laboratory setting, we should force the fluid to move on a curved surface with the shape of a double funnel as in Fig. 1. To find the exact required shape, we consider, in cylindrical coordinates, a surface parametrized by (R, θ) of the form

$$r = r(R), \quad \theta = \theta, \quad z = z(R), \tag{A2}$$

such that the induced metric on the surface

$$ds^2 = dr^2 + r^2 d\theta^2 + dz^2 = \left(\frac{\partial r(R)}{\partial R}\right)^2 dR^2 + r(R)^2 d\theta^2 + \left(\frac{\partial z(R)}{\partial R}\right)^2 dR^2 \tag{A3}$$

agrees with Eq. (A1). From this, we get the following equations:

$$\frac{dz(R)}{dR} = \frac{2\,R_0^2}{\sqrt{R^4 + R_0^4}}, \tag{A4}$$

$$r(R) = \sqrt{f(R)}R. \tag{A5}$$

The function $r(R)$ is determined and the equation for $z(R)$ can be integrated in terms of elliptic functions. Making a parametric plot of $r(R)$ and $z(R)$, we get the double-funnel geometry shown (with scaled out R_0) in Fig. 1. This shows that the metric is flat at $R \to \infty \Rightarrow r(R) \to \infty, z(R) > 0$, and $R \to 0 \Rightarrow r(R) \to \infty, z(R) < 0$. The span of the coordinate z is $\Delta z = z(R = +\infty) - z(R = 0) = \frac{R_0}{2}\frac{[\Gamma(\frac{1}{4})]^2}{\Gamma(\frac{1}{2})}$.

Another useful radial coordinate that respects the symmetry is $\xi = \frac{R}{R_0} - \frac{R_0}{R}$, with $-\infty < \xi < \infty$.

[1] W. G. Unruh, Experimental black-hole evaporation?, Phys. Rev. Lett. **46**, 1351 (1981).

[2] S. W. Hawking, Particle creation by black holes, Commun. Math. Phys. **43**, 199 (1975).

[3] C. Barceló, S. Liberati, and M. Visser, Analogue gravity, Living Rev. Relativ. **14**, 3 (2011).

[4] C. Barceló, S. Liberati, and M. Visser, Analogue gravity from Bose-Einstein condensates, Class. Quantum Grav. **18**, 1137 (2001).

[5] M. Visser, C. Barceló, and S. Liberati, Analogue models of and for gravity, Gen. Relativ. Gravit. **34**, 1719 (2002).

[6] L. J. Garay, J. R. Anglin, J. I. Cirac, and P. Zoller, Sonic analog of gravitational black holes in Bose-Einstein condensates, Phys. Rev. Lett. **85**, 4643 (2000).

[7] C. C. H. Ribeiro, S.-S. Baak, and U. R. Fischer, Existence of steady-state black hole analogs in finite quasi-one-dimensional Bose-Einstein condensates, Phys. Rev. D **105**, 124066 (2022).

[8] Z. Tian, Y. Lin, U. R. Fischer, and J. Du, Testing the upper bound on the speed of scrambling with an analogue of hawking radiation using trapped ions, Eur. Phys. J. C **82**, 212 (2022).

[9] P. O. Fedichev and U. R. Fischer, "Cosmological" quasiparticle production in harmonically trapped superfluid gases, Phys. Rev. A **69**, 033602 (2004).

[10] P. O. Fedichev and U. R. Fischer, Gibbons-Hawking effect in the sonic de sitter space-time of an expanding Bose-Einstein-Condensed gas, Phys. Rev. Lett. **91**, 240407 (2003).

[11] S. Vaidya and M. Kruczenski, Stationary acoustic black hole solutions in Bose-Einstein condensates and their Borel analysis, arXiv:2411.06678 [J. Phys. A (to be published)].

[12] S. Khlebnikov, Acoustic horizon as a phase-slip surface, Phys. Rev. A **109**, 023305 (2024).

[13] H. Tamura, S. Khlebnikov, C.-A. Chen, and C.-L. Hung, Observation of self-oscillating supersonic flow across an acoustic horizon in two dimensions, arXiv:2304.10667.

[14] J. Steinhauer, Observation of self-amplifying Hawking radiation in an analogue black-hole laser, Nat. Phys. **10**, 864 (2014).

[15] J. R. M. de Nova, K. Golubkov, V. I. Kolobov, and J. Steinhauer, Observation of thermal Hawking radiation and its temperature in an analogue black hole, Nature (London) **569**, 688 (2019).

[16] P. Nozieres and D. Pines, *The Theory of Quantum Liquids, Volume II: Superfluid Bose Liquids*, Advanced book Classics (Westview Press, USA, 1990), pp. 160–161.

[17] P. Nozieres and D. Pines, *The Theory of Quantum Liquids, Volume II: Superfluid Bose Liquids*, Advanced book Classics (Westview Press, USA, 1990), pp. 168–169.

[18] P. Nozieres and D. Pines, *The Theory of Quantum Liquids, Volume II: Superfluid Bose Liquids*, Advanced book Classics (Westview Press, USA, 1990), p. 66.

[19] R. D'Inverno, *Introducing Einstein's Relativity* (Oxford University Press, New York, 1992), pp. 88–89.

[20] J. Polchinski, *String Theory Volume I* (Cambridge University Press, 2000), p. 85.

[21] A. Saleh Taher, A. Malek, and S. Momeni-Masuleh, Chebyshev differentiation matrices for efficient computation of the eigenvalues of fourth-order Sturm-Liouville problems, Appl. Math. Model. **37**, 4634 (2013).

[22] A. Galántai, The theory of Newton's method, J. Comput. Appl. Math. **124**, 25 (2000), Numerical Analysis 2000, Vol. IV: Optimization and Nonlinear Equations.

[23] T. Na, *Computational Methods in Engineering Boundary Value Problems*, Mathematics in Science and Engineering (Academic Press, New York, 1979), p. 85.

[24] L. J. Garay, J. R. Anglin, J. I. Cirac, and P. Zoller, Sonic black holes in dilute Bose-Einstein condensates, Phys. Rev. A **63**, 023611 (2001).

[25] A. J. S. Hamilton and J. P. Lisle, The river model of black holes, Am. J. Phys. **76**, 519 (2008).

[26] L. Liao, E. C. I. van der Wurff, D. van Oosten, and H. T. C. Stoof, Proposal for an analog Schwarzschild black hole in condensates of light, Phys. Rev. A **99**, 023850 (2019).

[27] X. Liu, Z. Zhao, and W. Liu, Tortoise coordinate transformation on apparent horizon of a dynamical black hole, Int. J. Mod. Phys. Conf. Ser. **12**, 358 (2012).

[28] S. W. Hawking, Quantum gravity and path integrals, Phys. Rev. D **18**, 1747 (1978).